

Articles

Effect of Transition Metal(II)-N,N-Bis(salicylaldehyde)phenylenediimines on the Electrochemical Reduction of Thionyl Chloride

Hyun-Soo Kim, Yong-Kook Choi*, Ki-Hyung Chjo, Seong-Keun Kook, and Hee-Gweon Woo

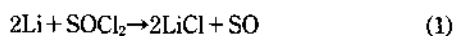
Department of Chemistry, Chonnam National University, Kwangju 500-757, Korea

Received March 14, 1995

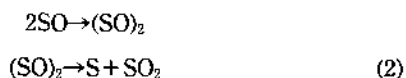
Catalytic effects of transition metal (Co^{2+} , Ni^{2+}) complexes of N,N-bis(salicylaldehyde)-*o*-phenylenediimine (SOPD), N,N-bis(salicylaldehyde)-*m*-phenylenediimine (SMPD), and N,N-bis(salicylaldehyde)-*p*-phenylenediimine (SPPD), on the reduction of thionyl chloride at glassy carbon electrode, are evaluated by determining the kinetic parameters with cyclic voltammetric technique. The charge transfer process for the reduction of thionyl chloride is strongly affected by the concentration of the catalysts. Some quadridentate Schiff base-M(II) complexes show sizable catalytic activities for the reduction of thionyl chloride. Catalytic effects of $[\text{M}(\text{II})(\text{SOPD})]$ complexes are slightly larger compared to $[\text{M}(\text{II})_2(\text{SMPD})_2]$ and $[\text{M}(\text{II})_2(\text{SPPD})_2]$ complexes. On those electrodes deposited with the catalysts, the observed exchange rate constants (k^0) are in the range of $0.89\text{--}2.28 \times 10^{-7}$ cm/s, while it is 1.24×10^{-8} cm/s on the bare glassy carbon electrode.

Introduction

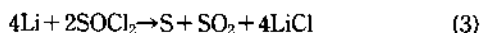
The lithium/thionyl chloride primary cell¹⁻²⁴ has received a considerable attention over the past several years because of its high power density and long shelf-life. The system consists of a Li anode, a porous carbon cathode, and a $\text{LiAlCl}_4/\text{SOCl}_2$ electrolyte, where SOCl_2 acts both as a solvent and as a cathode-active material. The Li anode is prevented from reacting with the SOCl_2 by virtue of the formation of a LiCl passivation film⁵ on the Li surface as soon as it contacts with the $\text{LiAlCl}_4/\text{SOCl}_2$ electrolyte according to the reaction (Eq. 1).



Dey²⁵ proposed that the unstable SO is dimerized and then disproportionated to $\text{S} + \text{SO}_2$ (Eq. 2).



The postulated reaction was therefore



The electrode kinetics of the cathodic discharge reaction are rather poor due to the formation of passive LiCl films at the electrode surface as a result of the reaction (3). The film is also the source of the voltage drop owing to its overly passive nature. Thus many investigators tried to avoid this high passivity problem. One approach to improve the cell performance can be the addition of catalyst molecules, which accelerates the rate of electron transfer.

Transition metal phthalocyanines, which have been successfully employed as catalysts for fuel cell cathodes, also improve the performance of lithium/thionyl chloride cell. Dodapaneni,¹⁹⁻²³ after testing eight metal complexes as possible catalysts, found cobalt and iron phthalocyanines to be most

effective. It has also been shown that adding a small amount of metal phthalocyanines improves cell performance. Choi and coworkers²⁴ observed the catalytic effects of cobalt phenylporphyrins on the thionyl chloride reduction.

In this paper, we report the results of catalytic effects of several Schiff base metal(II) complexes on the thionyl chloride reduction.

Experimental

The salicylaldehyde (Merck), *o*-phenylenediamine, *m*-phenylenediamine, *p*-phenylenediamine (Aldrich), Na_2CO_3 , $\text{Co}(\text{NO}_3)_2 \cdot 6\text{H}_2\text{O}$, $\text{Ni}(\text{NO}_3)_2 \cdot 6\text{H}_2\text{O}$, NaOH, and ethanol were used as received. The elemental analysis (carbon, hydrogen, and nitrogen) was performed on a Yanaco-CHN coder MT-3 analyzer, and the metal content was determined by a Perkin-Elmer model 603 atomic absorption spectrometer. Infrared and UV-vis spectra were recorded on Shimadzu IR-430 infrared and Hitachi-557 UV-vis spectrophotometers. Thermogravimetric analysis (TGA) was carried out using a Perkin-Elmer model 2 Thermogravimetric Analyzer. The ^1H NMR spectra in DMSO-d_6 were recorded by Bruker AMX-300 spectrometer.

Preparation of ligands

Typical procedures for ligand synthesis are as followed. A solution of 0.05 mole of phenylene diamine in 50 mL of ethanol was slowly added to 0.1 mole of salicylaldehyde in ethanol (50 mL) under the nitrogen atmosphere with stirring. After 2 hr at room temperature, precipitates were collected by filtration. The products were recrystallized from ethanol and dried under a reduced pressure at 80 °C.

N,N-bis(salicylaldehyde)-*o*-phenylenediimine, $[\text{H}_2\text{SOPD}]$. 98% yield; mp. 126-128 °C; Anal. Calcd for $\text{C}_{20}\text{H}_{16}\text{N}_2\text{O}_2$: C = 76.13, H = 5.03, N = 7.07, Found: C = 76.18, H = 5.00, N = 7.05; UV-vis (DMSO, λ_{max} , $\epsilon \times 10^{-4} \text{ cm}^{-1}\text{M}^{-1}$): 274 (4.55),

333 (3.89); IR (KBr pellet, cm^{-1}): 3425 (νOH), 1622 ($\nu\text{C}=\text{N}$); ^1H NMR (DMSO- d_6 , δ): 7.04 (m, ArH), 9.01 (s, $-\text{CH}=\text{N}-$), 13.02 (br, ArOH).

N,N-bis(salicylaldehyde)-m-phenylenedilimine, [H₂SMPD]. 95% yield; mp. 132-134 °C; Anal. Calcd for C₂₀H₁₆N₂O₂: C=76.13, H=5.03, N=7.07, Found: C=76.07, H=5.05, N=7.10; UV-vis (DMSO, λ_{max} , $\epsilon \times 10^{-4} \text{ cm}^{-1}\text{M}^{-1}$): 277 (4.28), 344 (4.37); IR (KBr pellet, cm^{-1}): 3429 (νOH), 1624 ($\nu\text{C}=\text{N}$); ^1H NMR (DMSO- d_6 , δ): 7.14 (m, ArH), 9.15 (s, $-\text{CH}=\text{N}-$), 13.12 (br, ArOH).

N,N-bis(salicylaldehyde)-p-phenylenedilimine, [H₂SPPD]. 97% yield; mp 141-143 °C; Anal. Calcd for C₂₀H₁₆N₂O₂: C=76.13, H=5.03, N=7.07, Found: C=76.10, H=4.99, N=7.09; UV-vis (DMSO, λ_{max} , $\epsilon \times 10^{-4} \text{ cm}^{-1}\text{M}^{-1}$): 278 (3.83), 374 (5.03); IR (KBr pellet, cm^{-1}): 3427 (νOH), 1617 ($\nu\text{C}=\text{N}$); ^1H NMR (DMSO- d_6 , δ): 7.21 (m, ArH), 9.21 (s, $-\text{CH}=\text{N}-$), 13.08 (br, ArOH).

Preparation of [M(II)(SOPD)(H₂O)₂] complexes

The complexes, [M(II)(SOPD)(H₂O)₂] (M=Co, Ni), were prepared by the addition of 0.01 mole H₂SOPD in ethanol to the same volume of 0.01 mole M(II)(NO₃)₂(H₂O)₆ (M=Co, Ni) in water under the nitrogen atmosphere. The precipitates were recrystallized from ethanol and dried at 80 °C under a reduced pressure.

[Co(II)(SOPD)(H₂O)₂]. 86% yield; mp 175-177 °C; Anal. Calcd for Co(II)(C₂₀H₁₈N₂O₄): C=58.69, H=4.43, N=6.85, Co=14.4, Found: C=58.9, H=4.41, N=6.83, Co=14.2; UV-vis (DMSO, λ_{max} , $\epsilon \times 10^{-4} \text{ cm}^{-1}\text{M}^{-1}$): 313 (4.63), 387 (4.13); IR (KBr pellet, cm^{-1}): 3439 (νOH), 1609 ($\nu\text{C}=\text{N}$), 756 ($\nu\text{Co-N}$), 545 ($\nu\text{Co-O}$); TGA (weight loss, %): 8.80 at 100-250 °C, 29.3 at 250-370 °C, 43.5 at 370-690 °C, 18.4 at 690 °C~.

[Ni(II)(SOPD)(H₂O)₂]. 87% yield; mp 165-167 °C; Anal. Calcd for Ni(II)(C₂₀H₁₈N₂O₄): C=58.71, H=4.44, N=6.85, Ni=14.35, Found: C=58.65, H=4.46, N=6.82, Ni=14.40. UV-vis (DMSO, λ_{max} , $\epsilon \times 10^{-4} \text{ cm}^{-1}\text{M}^{-1}$): 315 (3.39), 377 (4.04); IR (KBr pellet, cm^{-1}): 3452 (νOH), 1610 ($\nu\text{C}=\text{N}$), 750 ($\nu\text{Ni-N}$), 550 ($\nu\text{Ni-O}$); TGA (weight loss, %): 8.79 at 100-300 °C, 25.3 at 300-430 °C, 47.4 at 430-680 °C, 18.5 at 680 °C~.

Preparation of [M(II)₂(SMPD)₂(H₂O)₄] complexes

The complexes, [M(II)₂(SMPD)₂(H₂O)₄] (M=Co, Ni), were prepared by the addition of 0.01 mole H₂SMPD in ethanol to the same volume of 0.01 mole M(II)(NO₃)₂(H₂O)₆ (M=Co, Ni) in water under the nitrogen atmosphere. The precipitates were recrystallized from ethanol and dried at 80 °C under a reduced pressure.

[Co(II)₂(SMPD)₂(H₂O)₄]. 88% yield; mp 187-189 °C; Anal. Calcd for Co(II)₂(C₄₀H₃₆N₄O₈): C=58.69, H=4.43, N=6.85, Co=14.01, Found: C=58.73, H=4.37, N=6.91, Co=14.32; UV-vis (DMSO, λ_{max} , $\epsilon \times 10^{-4} \text{ cm}^{-1}\text{M}^{-1}$): 348 (3.15), 405 (2.32); IR (KBr pellet, cm^{-1}): 3445 (νOH), 1605 ($\nu\text{C}=\text{N}$), 754 ($\nu\text{Co-N}$), 552 ($\nu\text{Co-O}$); TGA (weight loss, %): 8.95 at 80-250 °C, 29.4 at 250-380 °C, 48.6 at 380-470 °C, 19.1 at 470 °C~.

[Ni(II)₂(SMPD)₂(H₂O)₄]. 85% yield; mp 201-203 °C; Anal. Calcd for Ni(II)₂(C₄₀H₃₆N₄O₈): C=58.72, H=4.44, N=6.85, Ni=14.35, Found: C=58.64, H=4.46, N=6.77, Ni=14.41; UV-vis (DMSO, λ_{max} , $\epsilon \times 10^{-4} \text{ cm}^{-1}\text{M}^{-1}$): 346 (3.44), 423 (1.24); IR (KBr pellet, cm^{-1}): 3443 (νOH), 1608 ($\nu\text{C}=\text{N}$),

722 ($\nu\text{Ni-N}$), 547 ($\nu\text{Ni-O}$); TGA (weight loss, %): 8.74 at 80-215 °C, 24.0 at 215-375 °C, 48.3 at 375-450 °C, 18.9 at 450 °C~.

Preparation of [M(II)₂(SPPD)₂(H₂O)₄] complexes

The complexes, [M(II)₂(SPPD)₂(H₂O)₄] (M=Co, Ni), were prepared by the addition of 0.01 mole H₂SPPD in ethanol to the same volume of 0.01 mole M(II)(NO₃)₂(H₂O)₆ (M=Co, Ni) in water under the nitrogen atmosphere. The precipitates were recrystallized from ethanol and dried at 80 °C under a reduced pressure.

[Co(II)₂(SPPD)₂(H₂O)₄]. 88% yield; mp 197-199 °C; Anal. Calcd for Co(II)₂(C₄₀H₃₆N₄O₈): C=58.69, H=4.43, N=6.85, Co=14.01, Found: C=58.62, H=4.46, N=6.90, Co=14.07; UV-vis (DMSO, λ_{max} , $\epsilon \times 10^{-4} \text{ cm}^{-1}\text{M}^{-1}$): 315 (2.51), 378 (2.98); IR (KBr pellet, cm^{-1}): 3437 (νOH), 1605 ($\nu\text{C}=\text{N}$), 758 ($\nu\text{Co-N}$), 540 ($\nu\text{Co-O}$); TGA (weight loss, %): 9.51 at 100-200 °C, 19.2 at 200-580 °C, 19.2 at 580 °C~.

[Ni(II)₂(SPPD)₂(H₂O)₄]. 85% yield; mp 205-208 °C; Anal. Calcd for Ni(II)₂(C₄₀H₃₆N₄O₈): C=58.72, H=4.44, N=6.85, Ni=14.35, Found: C=58.57, H=4.51, N=6.81, Ni=14.43; UV-vis (DMSO, λ_{max} , $\epsilon \times 10^{-4} \text{ cm}^{-1}\text{M}^{-1}$): 320 (2.13), 376 (3.78); IR (KBr pellet, cm^{-1}): 3449 (νOH), 1609 ($\nu\text{C}=\text{N}$), 750 ($\nu\text{Ni-N}$), 520 ($\nu\text{Ni-O}$); TGA (weight loss, %): 9.40 at 100-230 °C, 71.8 at 230-610 °C, 18.9 at 610 °C~.

Electrochemistry

Electrochemical reduction of thionyl chloride has been investigated by cyclic voltammetry techniques. Single electrochemical compartment cell, in which the glassy carbon working (geometric area, 0.071 cm^2), a platinum wire counter, and a lithium wire reference electrodes were housed, was used for the electrochemical measurement. Glassy carbon electrode was polished to a mirror finish with 1 μm alumina powder, subsequently cleaned in an ultrasonic cleaning bath for the removal of solid particles, and finally rinsed several times with doubly distilled water before use. The 1.53 M LiAlCl₄/SOCl₂ electrolytic solution (LITHCO) was used. All experiments were conducted in a glove box under the Ar atmosphere. A Princeton Applied Research (PAR) 273 potentiostat/galvanostat interfaced by 486 DX microcomputer through an IEEE-488 bus was used for cyclic voltammetry.

Results and Discussion

Quadridentate Schiff base Co(II) and Ni(II) complexes have been prepared and characterized by UV-vis, IR, TGA, NMR, and elemental analysis. The results of elemental analysis of the Schiff base ligand and their complexes are in good agreement with the expected composition of the proposed complexes (Figure 1 and 2).

The metal contents in the [M(II)(SOPD)], [M(II)₂(SMPD)₂], and [M(II)₂(SOPD)₂] complexes are also in good agreement with the proposed complexes. All complexes are insoluble in water but soluble in aprotic solvents and SOCl₂. It was observed from the thermogravimetric analysis of the complexes that hydrated water molecules are dried away at 80-250 °C and the metal oxides are formed at 450 °C.

IR spectra showed broad $\nu(\text{OH})$ bands of the Co(II) and Ni(II) complexes at 3440 cm^{-1} . The IR spectra showed that the Co(II) and Ni(II) complexes contain water molecules.²⁶

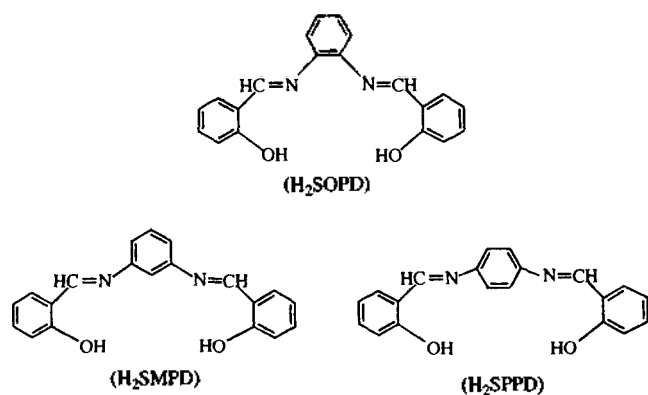


Figure 1. Structure of ligands.

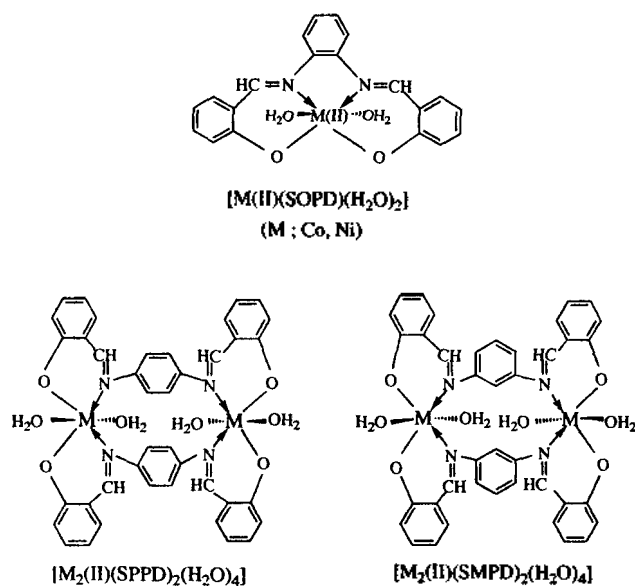
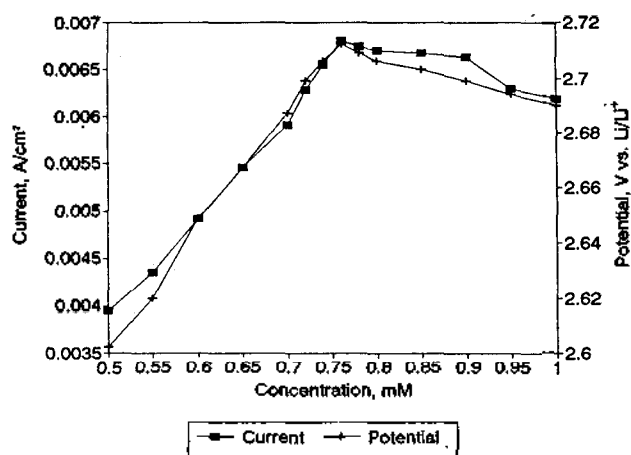
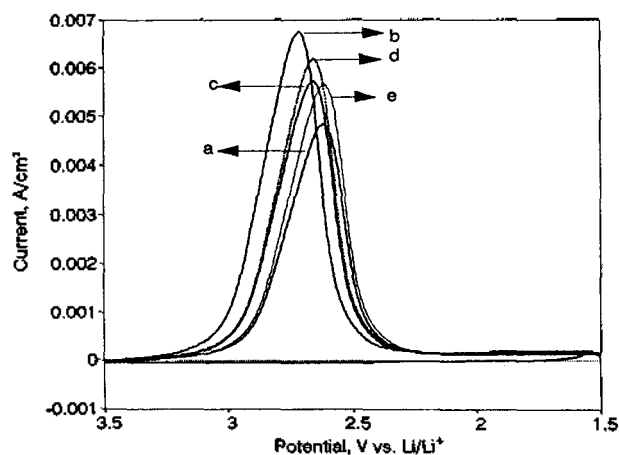


Figure 2. Structure of complexes.

The water molecules in the hydrated complexes may be in a strongly hydrogen bonded state, which may weaken the OH stretching vibration. One can also see that $\nu(C=N)$ bands in the complexes are shifted to the lower frequency regions of $1600-1610\text{ cm}^{-1}$ compared to the corresponding free ligands.²⁷ According to Ueno and Martell,²⁸ characteristic absorption bands for $M(II)-N$ and $M(II)-O$ bonds in the complexes appear in the spectral region of $650-850\text{ cm}^{-1}$ and $400-600\text{ cm}^{-1}$, respectively. Here two absorption bands at $720-760\text{ cm}^{-1}$ and $520-550\text{ cm}^{-1}$ are assigned to the $\nu(M(II)-N)$ and $\nu(M(II)-O)$ bands. The UV-vis spectra of the Co(II) and Ni(II) complexes obtained in DMSO solution showed a $\pi-\pi^*$ ligand field absorption band at $320-350\text{ nm}$ and a $d-\pi^*$ charge transfer band at $380-420\text{ nm}$. These observations are consistent with the proposed structure.

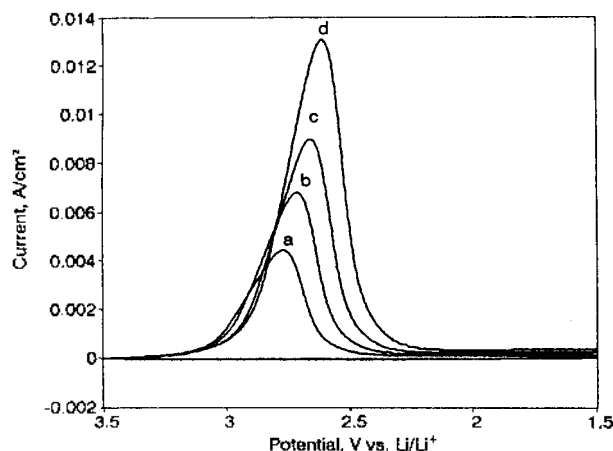
Catalytic effects of $[M(II)(SOPD)]$, $[M(II)_2(SMPD)_2]$, and $[M(II)_2(SPPD)_2]$ ($M = \text{Co, Ni}$) on the reduction of thionyl chloride at glassy carbon electrode are evaluated by determining the electrochemical kinetic parameters using cyclic voltammetry technique. Peak currents and peak potentials obtained from the cyclic voltammograms are plotted as a func-

Figure 3. Plots of the peak currents and peak potentials vs. the concentration of catalysts for the reduction of $SOCl_2$ solution containing $[Co(II)(SOPD)]$ at glassy carbon electrode. Scan rate was 50 mV/sec .Figure 4. Cyclic voltammograms for the reduction of $SOCl_2$ solution at optimum concentration containing: a) bare, b) $[Co(II)(SOPD)]$, c) $[Co(II)_2(SPPD)_2]$, d) $[Ni(II)(SOPD)]$, and e) $[Ni(II)_2(SPPD)_2]$. Scan rate was 50 mV/s .

tion of the catalyst concentration for $[Co(II)(SOPD)]$ complex (Figure 3). The magnitude of the reduction current appears to be strongly dependent on the catalyst concentration. This phenomenon has been observed for all $M(II)$ complexes studied, even though the catalytic effects are different. There is an optimal concentration for each catalyst at around $0.7-0.8\text{ mM}$ because the rate limiting step for the reduction of thionyl chloride depends on the electron transfer at electrode surface with the formation of large associates of Schiff base $M(II)$ complexes in the electrolyte.²⁹ It is clear that $[M(II)(SOPD)]$, $[M(II)_2(SMPD)_2]$, and $[M(II)_2(SPPD)_2]$ show sizable catalytic activities for the reduction of thionyl chloride. As Doddapaneni¹⁹ already pointed out, the fact implies that the catalyst molecules are adsorbed on the electrode surface first. The adsorbed molecules would be reduced on the electrode surface, which in turn reduces thionyl chloride resulting in a generation of oxidized catalyst molecules and thus com-

Table 1. Peak potentials and peak currents for the reduction of SOCl_2 at scan rate 50 mV/sec

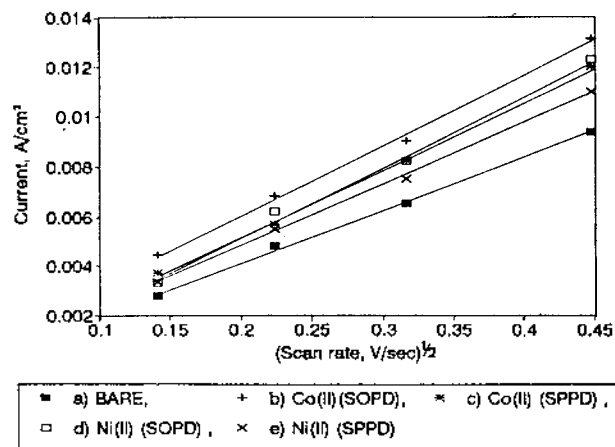
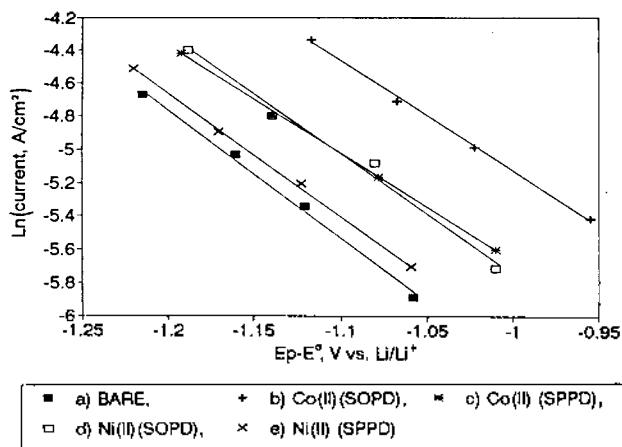
Catalysts	Concentration (mM)	Peak potential, E_p (V)	Peak current, i_p (mA/cm ²)
Bare	—	2.614	481
$\text{Co(II)(SOPD)(H}_2\text{O)}_2$	0.78	2.712	683
$\text{Ni(II)(SOPD)(H}_2\text{O)}_2$	0.80	2.654	617
$\text{Co(II)}_2(\text{SMPD})_2(\text{H}_2\text{O)}_4$	0.85	2.651	589
$\text{Ni(II)}_2(\text{SMPD})_2(\text{H}_2\text{O)}_4$	0.85	2.635	562
$\text{Co(II)}_2(\text{SPPD})_2(\text{H}_2\text{O)}_4$	0.80	2.656	571
$\text{Ni(II)}_2(\text{SPPD})_2(\text{H}_2\text{O)}_4$	0.80	2.612	545

**Figure 5.** Scan rate dependence of the voltammograms for the reduction of SOCl_2 solution containing 0.78 mM $[\text{Co(II)(SOPD)}]$ at glassy carbon electrode. Scan rates were a) 20, b) 50, c) 100, and d) 200 mV/s.

pletes the catalytic cycle.

Figure 4 shows cyclic voltammograms demonstrating the catalytic effect in thionyl chloride solution containing optimal concentration of $[\text{M(II)(SOPD)}]$ and $[\text{M(II)}_2(\text{SPPD})_2]$ complexes at glassy carbon electrode. The sharp current drops at negative potential side seem to be due to the passivation of the cathode by lithium chloride.¹¹ The catalytic effects are clearly seen by both the shift of the reduction potential toward positive direction (decrease of overpotential) and the increase of peak current. Peak currents and potentials observed for the reduction of thionyl chloride in the presence of catalysts are summarized in Table 1. The peak current increases and the potential shifts to positive direction. Therefore we conclude that these compounds show catalytic activities at glassy carbon electrode. As shown in Table 1, catalytic effects are larger for $[\text{M(II)(SOPD)}]$ as compared to $[\text{M(II)}_2(\text{SMPD})_2]$ and $[\text{M(II)}_2(\text{SPPD})_2]$ complexes due probably to the steric reason. Two metal sites in the $[\text{M(II)}_2(\text{SMPD})_2]$ and $[\text{M(II)}_2(\text{SPPD})_2]$ seem to hardly participate in the catalytic reaction.

Cyclic voltammetric experiments at an "optimum" catalyst concentration are conducted to evaluate kinetic parameters after waiting for some time until voltammograms develop to a well defined shape. Voltammograms were taken after

**Figure 6.** Plots of current vs. $v^{1/2}$ for the reduction of SOCl_2 at optimum concentration containing: a) bare, b) $[\text{Co(II)(SOPD)}]$, c) $[\text{Co(II)}_2(\text{SPPD})_2]$, d) $[\text{Ni(II)(SOPD)}]$, and e) $[\text{Ni(II)}_2(\text{SPPD})_2]$.**Figure 7.** Plots of $\ln(i_p)$ vs. $(E_p - E^0)$ for the reduction of SOCl_2 at optimum concentration containing: a) bare, b) $[\text{Co(II)(SOPD)}]$, c) $[\text{Co(II)}_2(\text{SPPD})_2]$, d) $[\text{Ni(II)(SOPD)}]$, and e) $[\text{Ni(II)}_2(\text{SPPD})_2]$.

the electrode was immersed into a fresh catalyst solution.

Figure 5 shows a series of cyclic voltammograms recorded at various scan rates ranging from 20–200 mV/sec in thionyl chloride solution containing 0.78 mM $[\text{Co(II)(SOPD)}]$. Figure 6 shows a plot of peak current vs. $v^{1/2}$ (v : scan rate) from voltammetric results obtained at glassy carbon electrode under the "optimum" conditions. This plot shows a linear relationship. The peak current from cyclic voltammetry in irreversible case is given as follow.³⁰

$$i_p = (2.99 \times 10^5) n(\alpha n_a)^{1/2} A C_o^* D_o^{1/2} v^{1/2} \quad (4)$$

where n is the number of electrons transferred, α the transfer coefficient, n_a the apparent number of electrons transferred, A the electrode area in cm^2 , C_o^* the bulk concentration of an electroactive compound in mole/ cm^3 , and D_o the diffusion coefficient of the electroactive compound or other charge carrier in cm^2/sec . Eq. (4) reveals that the plot of i_p vs. $v^{1/2}$ allows us to obtain the diffusion coefficient of thionyl chloride with known αn_a . From the relationship of between i_p and E_p ³⁰

Table 2. Kinetic parameters for the reduction of the SOCl_2 at scan rate 50 mV/sec

Catalysts	Concentration (mM)	αn_a	$AD_0^{1/2}$ ($\text{cm}^3/\text{s}^{1/2}$)	k^0 (cm/s)
Bare	—	0.14	6.40×10^{-6}	1.24×10^{-8}
$\text{Co(II)(SOPD)}_2(\text{H}_2\text{O})_2$	0.78	0.17	1.08×10^{-5}	2.28×10^{-7}
$\text{Ni(II)(SOPD)}_2(\text{H}_2\text{O})_2$	0.80	0.18	7.30×10^{-6}	1.04×10^{-7}
$\text{Co(II)}_2(\text{SMPD})_2(\text{H}_2\text{O})_4$	0.85	0.17	7.90×10^{-6}	1.26×10^{-7}
$\text{Ni(II)}_2(\text{SMPD})_2(\text{H}_2\text{O})_4$	0.85	0.20	6.90×10^{-6}	8.85×10^{-8}
$\text{Co(II)}_2(\text{SPPD})_2(\text{H}_2\text{O})_4$	0.80	0.15	8.10×10^{-6}	1.69×10^{-7}
$\text{Ni(II)}_2(\text{SPPD})_2(\text{H}_2\text{O})_4$	0.80	0.16	7.00×10^{-6}	7.14×10^{-8}

$$i_p = 0.227nFAC_0 k^0 \exp[-\{(an_a F)/(RT)\}(E_p - E^0)] \quad (5)$$

where k^0 is the exchange rate constant in cm/sec and E^0 is the formal potential in V. A plot of $\ln(i_p)$ vs. $E_p - E^0$ should yield a straight line with a slope, $\alpha n_a F/RT$, and an intercept, $\ln(0.227nFAC_0 k^0)$, from which αn_a and k^0 values can be calculated, respectively. In these calculation, the thermodynamic E^0 value of 3.72 V vs. Li is used as it is obtained from Eq. (3) using free energies of formation for reactants and products.⁸ The $\ln(i_p)$ vs. $(E_p - E^0)$ plots are shown in Figure 7 for the reduction of SOCl_2 at glassy carbon electrode in the presence of various catalysts. The αn_a value obtained from this equation can be used to determine $AD_0^{1/2}$ in Eq. (4). Kinetic parameters calculated from these plots at "optimum" catalyst concentrations are listed in Table 2. As shown in Table 2, $AD_0^{1/2}$ and exchange rate constant, k^0 , are determined to be $6.40 \times 10^{-6} \text{ cm}^3/\text{s}^{1/2}$ and $1.24 \times 10^{-8} \text{ cm/s}$ at bare glassy carbon electrode. These values at catalyst-supported glassy carbon electrode, however, are determined to be $10.8\text{--}7.00 \times 10^{-6} \text{ cm}^3/\text{s}^{1/2}$ and $0.89\text{--}2.28 \times 10^{-7} \text{ cm/s}$, respectively. The increases in exchange rate constant indicate a significant improvement in cell performance.

These results demonstrate that quadridentate Schiff base $[\text{M(II)(SOPD)}]$, $[\text{M(II)}_2(\text{SMPD})_2]$, and $[\text{M(II)}_2(\text{SPPD})_2]$ complexes show catalytic activities for the reduction of thionyl chloride. This can be the enhancement in the exchange rate constants. These result are in accordance with previous results reported by Doddapaneni¹⁹⁻²³ on the reduction of SOCl_2 solution containing metal phthalocyanine. Catalytic effects are greater in thionyl chloride solution containing Schiff base $[\text{M(II)(SOPD)}]$ as compared to $[\text{M(II)}_2(\text{SMPD})_2]$ and $[\text{M(II)}_2(\text{SPPD})_2]$ complexes.

Acknowledgment. This paper was supported in part by the Basic Science Research Institute Program, Ministry of Education of Korea (BSRI 94-3429), in part by NON DIRECTED RESEARCH FUND (1994), Korea Research Foundation.

References

1. Schlaikjer, C. R.; Goedel, F.; Marincic, N. *J. Electrochem.*

- Soc.* 1976, 126, 513.
2. Bowden, W.; Dey, A. N. *J. Electrochem. Soc.* 1979, 126, 2035.
3. Salmon, D. J.; Adamczyk, M. E.; Hendricks, L. L.; Abels, L. L.; Hall, J. C. in *Lithium Battery Technology*; Venkatesetty, H. V. Ed.; Proc. Electrochemical Society; Pennington, NJ., 1981.
4. Kolomoets, A. M.; Pleshakov, M. S.; Dudnikov, V. I. *Soviet Electrochem.* 1981, 17, 326.
5. Istone, W. K.; Brodd, R. J. *J. Electrochem. Soc.* 1982, 129, 1853.
6. Doddapaneni, N. *Proc. 30th Power Sources Symp.* The Electrochem. Soc.: Pennington, NJ., 1982.
7. Istone, W. K.; Brodd, R. J. *J. Electrochem. Soc.* 1984, 131, 2467.
8. Madou, M. J.; Szpak, S. *J. Electrochem. Soc.* 1984, 131, 2471.
9. Madou, M. J.; Smith, J. J.; Szpak, S. *J. Electrochem. Soc.* 1987, 134, 2794.
10. Chiu, J. G.; Wang, Y. Y.; Wany, C. C. *J. Power Sources* 1987, 21, 119.
11. Behl, K. *Proc. 27th Power Sources Symp.* The Electrochem. Soc. Pennington, NJ., 1976.
12. Hagan, W. P.; Hampson, N. A.; Packer, R. K. *J. Power Sources* 1988, 24, 95.
13. Hills, A. J.; Hampson, N. A. *J. Power Sources* 1988, 24, 253.
14. Mosier-Boss, P. A.; Szpak, S.; Smith, J. J.; Nowak, R. *J. J. Electrochem. Soc.* 1989, 136, 2455.
15. Bagotsky, V. S.; Kazarinov, V. E.; Volkovich, Yu. M.; Kanevsky, L. S.; Beketayeva, L. A. *J. Power Sources* 1989, 26, 427.
16. Hu, H. Y.; Ko, S. W. *J. Power Sources* 1989, 26, 419.
17. Schlaikjer, K. R. *J. Power Sources* 1989, 26, 161.
18. Choi, Y. K.; Kim, B. S.; Park, S. M. *J. Electrochem. Soc.* 1993, 140, 11.
19. Doddapaneni, N. *Proc. 30th Power Symp.* 1982, 169.
20. Doddapaneni, N. *Proc. 31th Power Symp.* 1984, 411.
21. Doddapaneni, N. *Proc. Electrochem. Soc.* 1982, 82-1, 591.
22. Doddapaneni, N. *Proc. Electrochem. Soc.* 1986, 86-12, 630.
23. Doddapaneni, N. *Proc. 32nd Power Symp.* 1986, 525.
24. Kim, W. S.; Choi, Y. K.; Chjo, K. H. *Bull. Korean Chem. Soc.* 1994, 15, 456.
25. Dey, A. N.; Bro, P. *J. Electrochem. Soc.* 1978, 125, 1574.
26. Ashmawy, F. M.; Issa, R. M.; Amer, S. A. *J. Chem. Soc. Dalton Trans.* 1986, 421.
27. Boucher, L. J. *Inorg. Chem.* 1976, 15, 1334.
28. Ueno, K.; Martell, A. E. *J. Phy. Chem.* 1956, 60, 1270.
29. Baturina, O. A.; Kanevsky, L. S.; Bagotzky, V. S.; Volodko, V. V.; Karasev, A. L.; Revina, A. A. *J. Power Sources* 1991, 36, 127.
30. Bard, A. J.; Faulkner, L. R. *Electrochemical methods*; Wiley: New York, 1980; Chap. 6.